PUBLICATIONS OF THE ASTRONOMICAL SOCIETY OF THE PACIFIC, **119**: 1085–1092, 2007 October

Metal Abundance Properties of M81 Globular Cluster System

JUN MA,[1] DAVID BURSTEIN,[2] ZHOU FAN,[1,3] XU ZHOU,[1] JIANSHENG CHEN,[1] ZHAOJI JIANG,[1] ZHENYU WU,[1] AND JIANGHUA WU[1]
Received 2007 June 1; accepted 2007 August 29; published 2007 October 25

ABSTRACT. This paper is the third in a series of papers on M81 globular clusters. In this paper, we present spatial and metal abundance properties of 95 M81 globular clusters, which comprise nearly half the entire M81 globular cluster system. These globular clusters are divided into two M81 metallicity groups by a KMM test. Our results show that the metal-rich clusters did not demonstrate a centrally concentrated spatial distribution the way the clusters in M31 do, and metal-poor clusters tend to be less spatially concentrated. In other words, the distribution of the metal-rich clusters in M81 is not very similar to that of M31. The quick histogram shows that most of the metal-rich clusters are distributed at projected radii of 4–8 kpc. Note also that the metal-rich clusters are distributed within the inner 20 kpc, and the metal-poor ones, out to radii of ~40 kpc. Like our Galaxy and M31, the metallicity distribution of globular clusters in M81 along a galactocentric radius suggests that some dissipation occurred during the formation of the globular cluster system; i.e., smooth, pressure-supported collapse models of galaxies are unlikely to produce the type of radial distribution of metallicity presented in this paper. There is no evident correlation between globular cluster luminosity and metallicity in M81 globular clusters. The overwhelming conclusion of this paper seems to be that a more complete and thorough cluster search is needed in M81.

1. INTRODUCTION

An understanding of galaxy formation and evolution is one of the principal goals of modern astrophysics. Globular clusters (GCs) are fossils of the earliest stages of galaxy formation and evolution. They are bright, easily recognized packages containing a stellar population with a homogeneous abundance and age. Thus, their integrated properties of location, abundance, and kinematics provide valuable clues to the nature and duration of galaxy formation (Barmby et al. 2000).

The metallicity distribution of globular clusters is of particular importance in deepening our knowledge of the dynamical and chemical evolution of the parent galaxies. For example, the globular clusters of many elliptical galaxies show multimodal metallicity distributions, suggesting that multiple star formation episodes occurred in these elliptical galaxies in the past (Zepf & Ashman 1993; Barmby et al. 2000). Great progress has been made in the past decade in our understanding of globular cluster systems of galaxies, especially the discovery that many galaxies possess two or more distinct subpopulations of globular clusters (e.g., West et al. 2004 and references therein). Based on the data from the *Hubble Space Telescope* (*HST*) archive, Gebhardt & Kissler-Patig (1999), Larsen et al. (2001), and Kundu & Whitmore (2001) showed that many large galaxies possess two or more subpopulations of globular clusters that have quite different chemical compositions. Recently, Peng et al. (2006) presented the color distributions of globular cluster systems for 100 early-type galaxies observed in the Virgo Cluster Survey with the Advanced Camera for Surveys (ACS) on *HST* and found that, on average, galaxies at all luminosities in their study appear to have bimodal or asymmetric GC color/metallicity distributions. The presence of color bimodality indicates that there have been at least two major star-forming mechanisms in the histories of galaxies.

Côté (1999) presented a metallicity distribution of 133 Galactic globular clusters that apparently shows two peaks (i.e., two distinct metal-poor and metal-rich globular cluster populations). A double Gaussian can best fit these two subpopulations; the mean metallicity values are -1.59 and -0.55 dex, respectively. Using the data for 247 globular clusters in M31, Barmby et al. (2000) studied the metallicity distribution, which is asymmetric, implying the possibility of bimodality. Then they applied a KMM algorithm (Ashman et al. 1994) showing that the metallicity distribution is really bimodal. Perrett et al. (2002) confirmed the conclusions of Barmby et al. (2000). Ma et al. (2005) showed that the intrinsic B and V colors and metallicities of 94 M81 globular clusters are bimodal, with metallicity peaks at [Fe/H] ≈ -1.45 and -0.53, similar to what we find for the Milky Way and M31 globular clusters.

M81 is one of the nearest Sa/Sb-type spirals outside the Local Group, very similar to M31 and roughly as massive as the Milky Way. Thus, beyond the Local Group, it is a good candidate for achieving a detailed study of a spiral galaxy globular

[1] National Astronomical Observatories, Chinese Academy of Sciences, Beijing, China; majun@vega.bac.pku.edu.cn.
[2] Department of Physics and Astronomy, Arizona State University, Tempe, AZ.
[3] Graduate University of Chinese Academy of Sciences, Beijing, China.

cluster system for comparison to the Milky Way and M31 system. Brodie & Huchra (1991) derived spectroscopic metallicities for eight globular clusters in M81 and presented the sample mean of [Fe/H] = −1.46 ± 0.31. Perelmuter et al. (1995) obtained low signal-to-noise ratio spectra of 82 candidates, 25 of which were confirmed as bona fide M81 globular clusters. They derived the mean metallicity to be [Fe/H] = −1.48 ± 0.19 both from the weighted mean of the individual metallicities and directly from the composite spectrum of the 25 confirmed globular clusters. To maximize the success rate of the globular cluster candidate list for the ongoing spectroscopic observations, Perelmuter & Racine (1995) used an extensive database that included photometric, astrometric, and morphological information on 3774 objects covering over a >50′ diameter field centered on M81 to reveal 70 globular cluster candidates.

Schroder et al. (2002) presented moderate-resolution spectroscopy for 16 globular cluster candidates from the list in Perelmuter & Racine (1995) and confirmed these 16 candidates as bona fide globular clusters. They also obtained metallicities for 15 of the 16 globular clusters. From their results, Schroder et al. (2002) concluded that the M81 globular cluster system is very similar to the Milky Way and M31 systems, both chemically and kinematically.

With the superior resolution of the *HST*, M81 is close enough for its clusters to be easily resolved on the basis of image structure (Chandar et al. 2001). Thus, using the *B*, *V*, and *I* bands of the *HST* Wide Field Planetary Camera 2 (WFPC2), Chandar et al. (2001) imaged eight fields covering a total area of ∼40 arcmin^2 and detected 114 compact star clusters in M81, 59 of which are globular clusters. Based on the estimated intrinsic colors, Chandar et al. (2004) found that the M81 globular cluster system has an extended metallicity distribution, which argues the presence of both metal-rich and metal-poor globular clusters. Ma et al. (2005) then confirmed this conclusion.

The outline of the paper is as follows. In § 2 we provide some statistical relationships. The summary is presented in § 3.

2. PROPERTIES OF GLOBULAR CLUSTERS IN M81

2.1. Sample of Globular Clusters

In the first paper of our series, Ma et al. (2005) studied the distributions of intrinsic *B* and *V* colors and metallicities of 95 M81 globular clusters, which are from Perelmuter et al. (1995), Chandar et al. (2001), and Schroder et al. (2002). This cluster sample includes nearly half of the M81 total GC population—a total that Perelmuter & Racine (1995) estimated as 210 ± 30 by *BVR* photometric, astrometric, and image structure study of the M81 field and Chandar et al. (2001) estimated as 211 ± 29 using GC estimates in various annular bins and correcting for incompleteness. It was difficult to detect and confirm GCs beyond the Local Group before *HST* appeared. In fact, even in the Local Group, it is also not easy to detect and confirm GCs. For example, Barmby & Huchra (2001) estimated the total number of GCs in M31 to be 460 ± 70; the largest number of GCs used to study the metal abundance properties of the M31 GCs includes 301 clusters collected by Perrett et al. (2002), a little more than half of the total number. Beyond the Local Group, the GC sample in M81 collected by Ma et al. (2005) includes the largest number of GCs compared to the total GCs in the host galaxy.

In the second paper of our series, Ma et al. (2006) presented the spectral energy distributions of 42 M81 globular clusters selected from Ma et al. (2005) in 13 intermediate-band filters from 4000 to 10,000 Å, using the CCD images of M81 observed as part of the Beijing-Arizona-Taiwan-Connecticut (BATC) multicolor survey of the sky, and confirmed the conclusions of Schroder et al. (2002) that M81 contains clusters as young as a few gigayears, which were also observed in both M31 and M33. In this paper, we study the spatial and metal abundance properties of the M81 GCs using the sample GCs of Ma et al. (2005). Figure 1 is the image of M81 in filter BATC07 (5785 Å) of the BATC multicolor survey of the sky; the circles indicate the positions of the sample clusters.

As mentioned above, Ma et al. (2005) studied the distributions of the intrinsic *B* and *V* colors and metallicities of these 95 M81 globular clusters and were the first to find that the abundance distribution of the GC system is consistent with a bimodal distribution with peaks at [Fe/H] ≈ −1.45 and −0.53 based on the KMM algorithm of Ashman et al. (1994). It is true that the appearance of the histogram can be ambiguous and misleading with binned data; however, the KMM algorithm of Ashman et al. (1994) is a robust method of analysis without relying on binning methods (see Perrett et al. 2002). KMM mixture modeling works under the assumption that the sample data are independently drawn from a parent population that comprises a mixture of *N* Gaussian distributions. Ma et al. (2005) presented that, for M81 globular clusters, the a posteriori probabilities of group membership returned by the KMM algorithm assigned 74 clusters to the metal-poor population and 20 to the metal-rich population distribution.[4]

2.2. Spatial Distribution

Figure 2 shows the projected spatial distributions of the metal-poor and metal-rich globular clusters in M81. We adopt an M81 distance modulus of 27.8 (Freedman et al. 1994; Chandar et al. 2001). We adopt M81 inclination and position angles of 59° and 157°, respectively, as Chandar et al. (2001) did. When the line of intersection (i.e., the major axis of the image) between the galactic plane and tangent plane is taken as the

[4] Since globular cluster 96 of Chandar et al. (2001) has very high $(B-V)_0$ [$(B-V)_0 = 1.778$] and the metallicity obtained using the color-metallicity correlation is too rich (0.95 dex), Ma et al. (2005) do not include it when performing the KMM test.

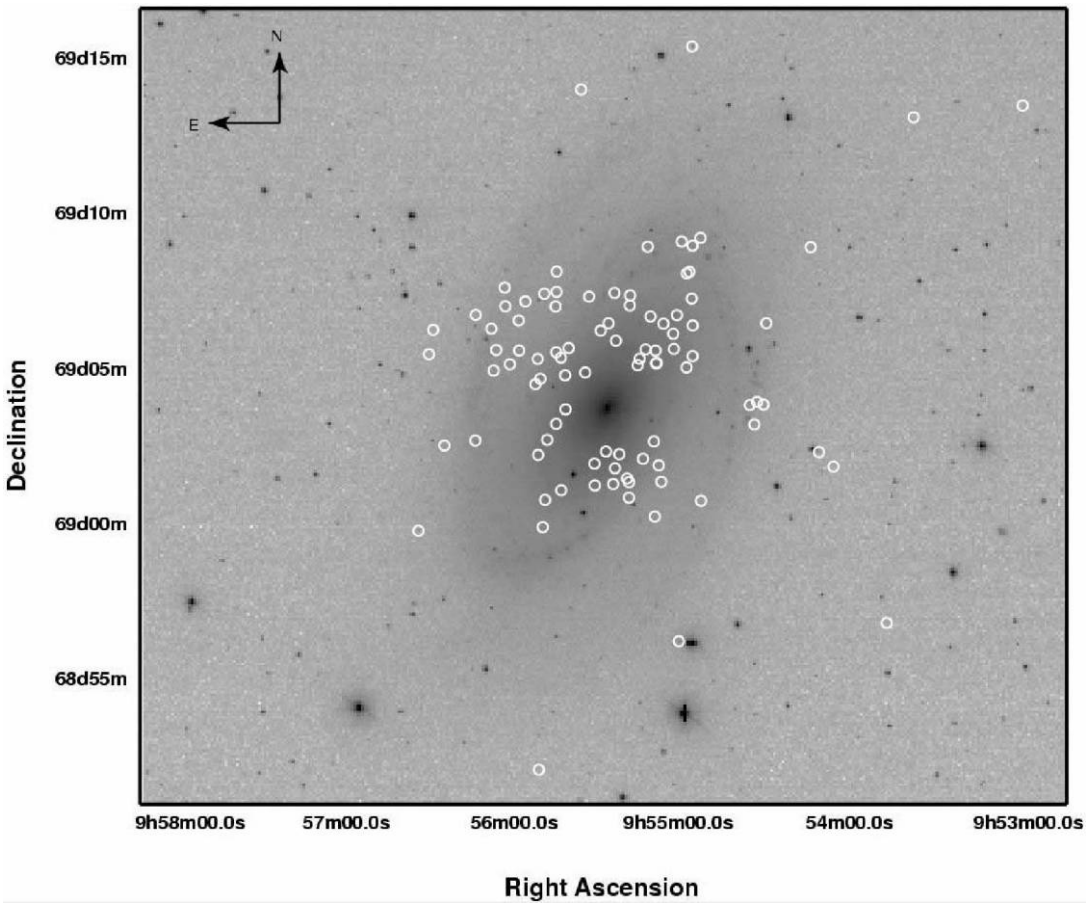

FIG. 1.—Image of M81 in filter BATC07 (5785 Å) and the positions of the sample star clusters. The center of the image is located at R.A. = $01^h33^m50.58^s$, decl. = $30°39'08.4''$ (J2000.0). North is up and east is to the left.

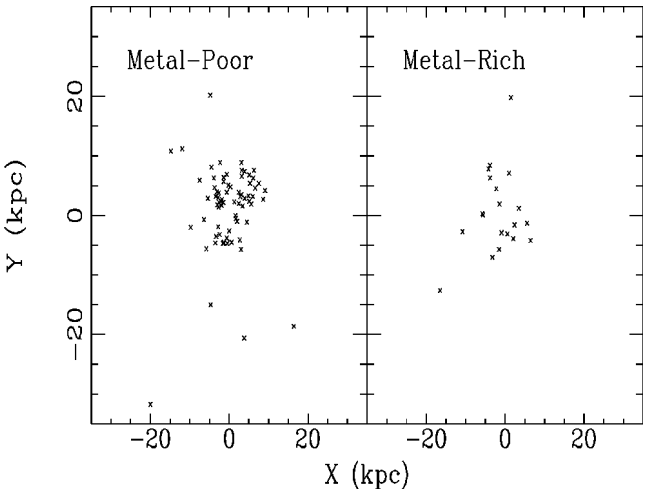

FIG. 2.—Spatial distributions of the metal-rich and metal-poor globular clusters.

polar axis, it is easily proved that

$$r = \rho\sqrt{1 + \tan^2\gamma \sin^2\theta}, \tag{1}$$

$$\tan\phi = \frac{\tan\theta}{\cos\gamma}, \tag{2}$$

where r and ϕ are the polar coordinates in the galactic plane, ρ and θ are the corresponding coordinates in the tangent plane, and γ is the inclination angle of the galactic disk. Using equation (1), we can obtain the distances of our sample clusters from the center of M81, which are listed in Table 1. In Table 1 we also list the metallicities of the sample clusters from Ma et al. (2005). From Figure 2, it is clear that the metal-rich GCs in M81 are not as centrally concentrated as the metal-rich GCs of M31 are (Huchra et al. 1991; Perrett et al. 2002). Figure 3 presents the histogram for the metal-poor and metal-rich GCs in M81. It shows that most of the metal-rich clusters are distributed at projected radii of 4–8 kpc. Note also that the metal-rich clusters are

TABLE 1
GLOBULAR CLUSTER SAMPLE AND PROPERTIES

ID[a]	[Fe/H]	Distance from M81 Center (kpc)	ID[a]	[Fe/H]	Distance from M81 Center (kpc)
Id30244	−1.53 ± 0.072	24.9	CFT5	−0.87 ± 0.070	8.5
Is40083	−1.29 ± 0.80	39.4	CFT6	−1.40 ± 0.084	8.4
Is40165	−1.57 ± 0.43	20.7	CFT8	−0.90 ± 0.060	7.3
Is40181	−0.76 ± 0.072	19.9	CFT15	−1.81 ± 0.314	9.9
Is50037	−2.34 ± 0.83	15.7	CFT16	−1.53 ± 0.360	8.8
Is50225	−0.04 ± 0.59	7.7	CFT20	−1.46 ± 0.205	8.0
Is50233	−1.23 ± 0.072	6.5	CFT21	−1.50 ± 0.263	9.3
Is50286	−1.45 ± 0.072	8.1	CFT22	−0.70 ± 0.253	7.3
Id50357	−0.33 ± 0.072	11.1	CFT28	−1.24 ± 0.393	7.4
Is50394	−2.17 ± 0.072	10.0	CFT30	−1.09 ± 0.128	9.3
Id50401	−0.72 ± 0.072	5.7	CFT31	−0.54 ± 0.502	8.9
Id50415	−1.90 ± 0.71	4.6	CFT32	−0.08 ± 0.205	9.2
Id50696	−1.86 ± 0.50	3.5	CFT34	−1.25 ± 0.174	9.2
Id50785	−1.58 ± 0.072	6.1	CFT37	−1.80 ± 0.031	3.2
Is50861	−1.38 ± 0.072	6.0	CFT38	−1.44 ± 0.029	3.2
Is50886	−1.79 ± 0.87	6.9	CFT39	−1.29 ± 0.022	3.4
Id50960	−1.79 ± 0.64	9.4	CFT41	−1.59 ± 0.022	3.1
Is51027	−2.06 ± 0.072	9.5	CFT42	−1.52 ± 0.034	2.6
Is60045	−1.03 ± 0.97	20.9	CFT43	−1.62 ± 0.138	2.6
Id70319	−1.00 ± 0.072	16.3	CFT44	−1.61 ± 0.123	4.1
Id70349	−1.19 ± 0.072	18.3	CFT45	−1.63 ± 0.043	5.1
Is80172	−0.77 ± 0.68	20.7	CFT46	−1.66 ± 0.051	4.7
Is90103	−2.23 ± 0.99	37.5	CFT49	−1.67 ± 0.191	4.6
SBKHP1	−1.207 ± 0.369	4.9	CFT51	−0.35 ± 0.084	5.1
SBKHP2	−0.707 ± 0.167	4.5	CFT53	−1.81 ± 0.058	6.5
SBKHP3	−0.211 ± 0.193	3.2	CFT56	−1.63 ± 0.034	3.8
SBKHP4	−0.407 ± 0.088	2.9	CFT58	0.21 ± 0.343	3.7
SBKHP5	−1.086 ± 0.091	2.2	CFT62	−1.11 ± 0.017	4.6
SBKHP6	−1.493 ± 0.206	1.7	CFT63	−1.69 ± 0.628	4.2
SBKHP7	−0.955 ± 0.098	1.6	CFT65	−1.87 ± 0.080	2.7
SBKHP8	−0.698 ± 0.058	2.4	CFT66	−1.85 ± 0.077	4.7
SBKHP9	−1.212 ± 0.133	2.7	CFT67	−1.31 ± 0.092	3.1
SBKHP10	−1.322 ± 0.356	4.0	CFT68	−1.62 ± 0.060	4.9
SBKHP11	−1.114 ± 0.409	4.8	CFT74	−1.72 ± 0.060	5.9
SBKHP12	−1.06 ± 0.072	5.1	CFT75	−1.64 ± 0.046	5.6
SBKHP13	−1.055 ± 0.062	7.6	CFT76	−1.87 ± 0.046	5.9
SBKHP14	−1.107 ± 0.074	5.9	CFT80	−1.79 ± 0.152	6.8
SBKHP15	−1.014 ± 0.713	8.2	CFT83	−1.63 ± 0.282	10.0
SBKHP16	−0.674 ± 0.044	7.1	CFT85	−1.61 ± 0.203	9.0
CFT87	−0.66 ± 0.087	5.9	FT106	−0.93 ± 0.147	4.7
CFT90	−0.51 ± 1.733	5.6	FT108	−1.00 ± 0.123	3.8
CFT96	0.95 ± 0.792	6.2	FT109	−0.50 ± 0.234	3.1
CFT97	−1.22 ± 0.056	6.4	FT110	−1.29 ± 0.215	2.6
FT101	−1.44 ± 0.386	5.0	FT111	−1.14 ± 0.150	4.7
FT102	0.01 ± 0.659	5.9	FT112	−1.79 ± 0.256	4.5
FT103	−1.65 ± 0.263	5.8	FT113	−0.68 ± 0.140	7.7
FT104	−1.30 ± 0.082	4.8	FT114	−1.73 ± 0.159	3.4
FT105	−1.02 ± 0.075	4.0			

[a] SBKHP identifications are from Schroder et al. (2002); CFT identifications are from Chandar et al. (2001); the others are from Perelmuter et al. (1995).

distributed within the inner 20 kpc, and the metal-poor ones are out to radii of ∼40 kpc. In the Milky Way, the metal-rich GCs reveal significant rotations and have historically been associated with the thick-disk system (Zinn 1985; Armandroff 1989); however, other works (Frenk & White 1982; Minniti 1995; Côté 1999; Forbes et al. 2001) have suggested that metal-rich GCs within ∼5 kpc of the Milky Way Galactic center are better associated with the bulge and bar. In M31, Elson & Walterbos (1988) showed that the metal-rich clusters constitute a more highly flattened system than the metal-poor ones and appear to have disklike kinematics; Huchra et al. (1991) showed that the metal-rich GCs are preferentially close to the galaxy center.

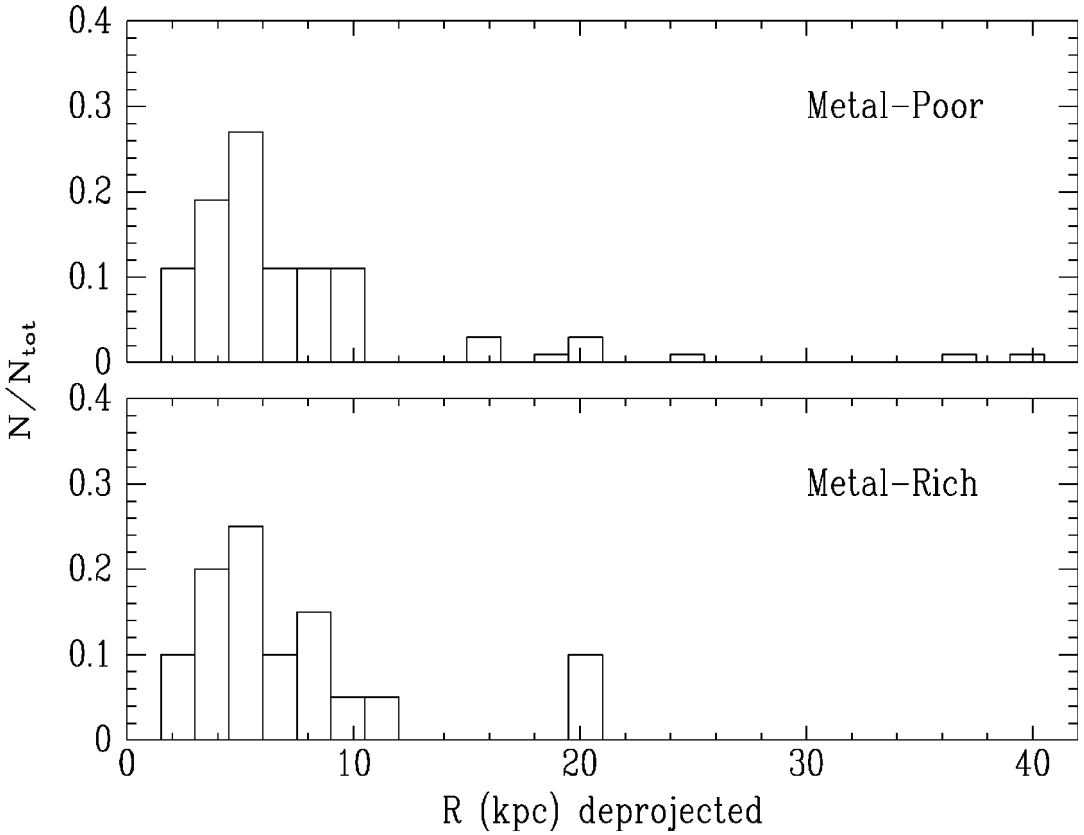

FIG. 3.—Radial distributions of the metal-rich and metal-poor globular clusters.

At the same time, Huchra et al. (1991) showed that the distinction between the rotation of the metal-rich and metal-poor clusters is most apparent in the inner 2 kpc. Thus, Huchra et al. (1991) concluded that the metal-rich clusters in M31 appear to form a central rotating disk system. With the largest sample of 321 velocities, Perrett et al. (2002) provided a more comprehensive investigation on the kinematics of the M31 cluster system. Perrett et al. (2002) showed that the metal-rich globular clusters of M31 appear to constitute a distinct kinematic subsystem that demonstrates a centrally spatial distribution with a high rotation amplitude but does not appear significantly flattened, which is consistent with a bulge population. It is of interest to mention that Schroder et al. (2002) performed a maximum likelihood kinematic analysis on 166 M31 clusters of Barmby et al. (2000) and found that the most significant difference between the rotation of the metal-rich and metal-poor clusters occurs at intermediate projected galactocentric radii. In particular, Schroder et al. (2002) presented a potential thick-disk population among M31's metal-rich globular clusters. For M81 globular clusters, Schroder et al. (2002) performed a kinematic analysis of the velocities of 44 M81 globular clusters and strongly suggested that the metal-rich clusters are rotating in the same sense as the gas in the disk of M81. Schroder et al. (2002) concluded that although their cluster sample is not large enough to make a direct comparison between metal-rich and metal-poor clusters in specific radius ranges, the conclusion that M81's metal-rich clusters at intermediate projected radii are associated with a thick disk in M81 is correct. It is true that, from Figure 3, most metal-rich clusters are distributed at projected radii of 4–8 kpc. Thus, we can at least conclude that most of the metal-rich clusters in our sample are not associated with a bulge cluster system of M81; they may be associated with a thick disk in M81 as indicated by Schroder et al. (2002). The sample clusters of this paper include all the sample clusters of Schroder et al. (2002). However, except for the sample clusters of Schroder et al. (2002), the clusters have no published radial velocity estimates. Thus, obviously, more kinematic and metallicity data are needed for globular clusters in M81 to determine whether the inner metal-rich GCs have kinematic properties that are consistent with a bulge and the metal-rich GCs at projected radii of 4–8 kpc are associated with a thick disk in M81.

2.3. Metallicity Gradient

The presence or absence of a radial trend in globular cluster metallicities is an important test of galaxy formation theory (Barmby et al. 2000). If a galaxy forms as a consequence of

a monolithic dissipative and rapid collapse of a single massive, nearly spherical spinning gas cloud in which the enrichment timescale is shorter than the collapse time, the halo stars and globular clusters should show large-scale metallicity gradients (Eggen et al. 1962; Barmby et al. 2000); however, Searle & Zinn (1978) have presented a chaotic scheme in the early evolution of a galaxy, in which loosely bound preenriched fragments merge with the main body of the protogalaxy over a significant period, so there should be a homogeneous metallicity distribution. For the Milky Way, Armandroff (1989) have showed some evidence that metallicity gradients with both distance from the Galactic plane and distance from the Galactic center were present in the disk cluster system. For M31, there are some inconsistent conclusions, such as van den Bergh (1969) showing that there is little or no evidence for a correlation between metallicity and projected radius, but most of his clusters were inside 50′; however, some authors (see, e.g., Huchra et al. 1982, 1991; Sharov 1988; Perrett et al. 2002) have presented evidence for a weak but measurable metallicity gradient as a function of projected radius. Barmby et al. (2000) confirmed the latter result based on their large sample of spectral metallicity and color-derived metallicity. Figure 4 plots the metallicity of the M81 globular clusters as a function of galactocentric radius; filled circles indicate the clusters with spectroscopic metallicities with uncertainties smaller than 1.0 dex. Clearly, the dominant feature of this diagram is the scatter in metallicity at any radius. At the same time, our sample clusters are mainly distributed in the inner 10 kpc. Thus, it is difficult to determine the metallicity gradient. It is true that smooth, pressure-supported collapse models of galaxies are unlikely to produce a result like this. However, in order to present a quantitative conclusion, we made least-squares fits: the total sample of globular clusters does not have a significant metallicity gradient (-0.009 ± 0.009 dex kpc^{-1}), and the clusters with spectroscopic metallicities with uncertainties smaller than 1.0 dex have a marginally significant gradient (-0.018 ± 0.01 dex kpc^{-1}). This result is in agreement with Kong et al. (2000), who obtained metallicity maps of the M81 field by comparing simple stellar population synthesis models of BC96 (G. Bruzual & S. Charlot 1996, unpublished) with the integrated photometric measurements of the BATC photometric system and did not find, within their errors, any obvious metallicity gradient from the central region to the bulge and disk of M81. However, we should emphasize that in the least-squares fits of this paper, the metal-rich clusters seem to play an important part in determining the metallicity gradient. From Figure 4, we can also see the decrease in the "upper envelope" of metallicity reported by Huchra et al. (1991) and Barmby et al. (2000) for M31 globular clusters. In fact, when we do a least-squares fit for the metal-poor clusters of M81, the metallicity gradient is -0.006 ± 0.006 dex kpc^{-1}. This metallicity gradient may not have any statistical meaning. It is clear that the small sample of metal-rich clusters in M81 cannot present any firm conclusion about metallicity gradient.

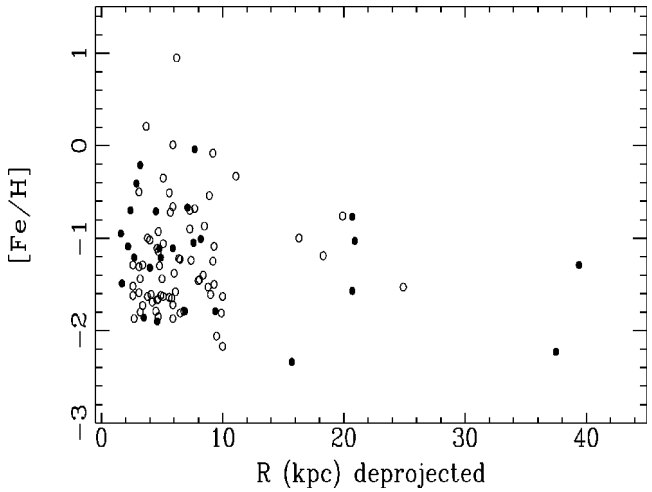

FIG. 4.—Metallicity as function of projected radius for M81 globular clusters. Filled circles indicate the clusters with spectroscopic metallicities with uncertainties smaller than 1.0 dex.

2.4. Metallicity versus Absolute Magnitude

The correlation between cluster mass (or luminosity) and metallicity is important in globular cluster formation theory. It is generally believed that if self-enrichment is important in GCs, the most massive clusters could retain their metal-enriched supernova ejecta, so the metal abundance should increase with cluster mass; the opposite is true if cooling from metals determines the temperature in the cluster-forming clouds (Barmby et al. 2000). The self-enrichment of GCs has been studied in detail in some aspects (for details, see Strader et al. 2006). However, it is interesting to mention the model of GC self-enrichment developed by Parmentier et al. (1999). In this model, cold and dense clouds embedded in the hot protogalactic medium are assumed to be the progenitors of galactic halo GCs. Based on this model, Parmentier & Gilmore (2001) showed that the most metal-rich proto–globular clusters are the least massive ones.

For M31 globular clusters, Huchra et al. (1991) first presented the metallicity versus apparent magnitude for 150 M31 clusters and did not find any trend of metallicity with luminosity; then, Barmby et al. (2000) showed metallicity versus dereddened apparent magnitude using a large cluster sample including 247 objects and confirmed the conclusion of Huchra et al. (1991).

Figure 5 shows metallicity versus absolute magnitude for M81 globular clusters; filled circles indicate the clusters with spectroscopic metallicities with uncertainties smaller than 1.0 dex. The metallicity and absolute magnitudes for the sample clusters are from Ma et al. (2005). It is true that there is no obvious trend of metallicity with luminosity as M31 GCs show. Least-squares fits show no evidence for a relationship between luminosity and metallicity in M81 clusters.

As we know, *HST* provides a unique tool for studying glob-

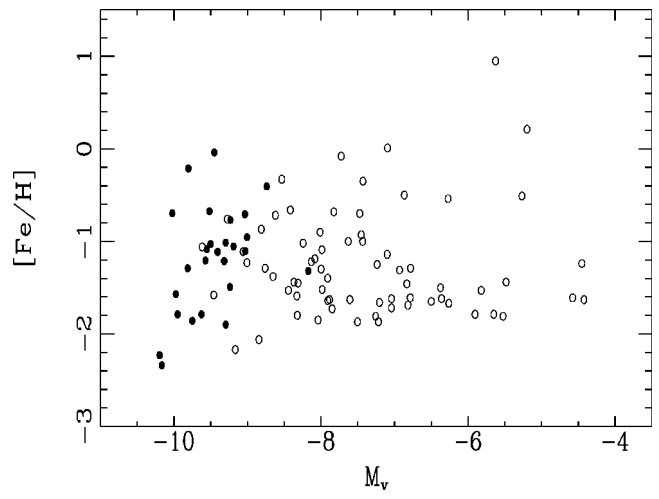

FIG. 5.—Same as Fig. 4, but for metallicity vs. absolute magnitude.

ular clusters in other galaxies. Recently, based on *HST* ACS data, Harris et al. (2006), Mieske et al. (2006), and Strader et al. (2006) found that in giant ellipticals such as M87, NGC 4649, and NGC 7094, luminous blue GCs (i.e., metal-poor GCs) reveal a trend of having redder colors, such that more massive GCs are more red (metal-rich). This trend is referred to as a "blue tilt" (see also Brodie & Strader 2006). This blue tilt was interpreted as a result of self-enrichment (Strader et al. 2006). Strader et al. (2006) speculatively suggested that these GCs once possessed dark matter halos. Spitler et al. (2006) subsequently found that this blue tilt is also present in the Sombrero spiral galaxy (NGC 4594) and may extend to less luminous GCs with a somewhat shallower slope that was derived by Harris et al. (2006) and Strader et al. (2006). As Spitler et al. (2006) pointed out, the Sombrero provides the first example of this trend in a spiral galaxy and in a galaxy found in a low-density galaxy environment. However, in these ACS studies, the metal-rich (red) GCs did not show this corresponding trend (also see Bekki et al. 2007). Based on high-resolution cosmological simulation with globular clusters, Bekki et al. (2007) investigated formation processes and physical properties of GC systems in galaxies and found that luminous metal-poor clusters would show a correlation between luminosity and metallicity if they originated from nuclei of low-mass galaxies at high z. In fact, in the simulations of Bekki et al. (2007) the "simulated blue tilts" emerge from the assumption that luminous metal-poor clusters originate from stellar galactic nuclei of the more massive nucleated galaxies with a luminosity-metallicity relation. Thus, it is evident that in Bekki et al. (2007) galaxies that experienced more accretion/merging events of nucleated low-mass galaxies are more likely to show a blue tilt (see details in Bekki et al. 2007).

3. SUMMARY

In this paper we present spatial and metal abundance properties of 95 M81 globular clusters, which are collected by Ma et al. (2005). This cluster sample includes nearly half of the M81 total globular cluster population and is the largest one making a comparison with the total globular clusters of the host galaxy beyond the Local Group. Our conclusions are as follows:

1. The metal-rich clusters did not demonstrate a centrally concentrated spatial distribution like that found in M31, and metal-poor clusters tend to be less spatially concentrated. Most metal-rich clusters are distributed at projected radii of 4–8 kpc. We can conclude that most of the metal-rich clusters in our sample are not associated with a bulge cluster system of M81; they may be associated with a thick disk in M81 as indicated by Schroder et al. (2002).

2. The globular clusters in M81 have a small radial metallicity gradient like M31 and our Galaxy, suggesting that some dissipation occurred during the formation of the globular cluster system.

3. There is no obvious trend of metallicity with luminosity in M81 globular clusters.

We are indebted to the referee for thoughtful comments and insightful suggestions that improved this paper greatly. This work has been supported by Chinese National Natural Science Foundation grants 10473012, 10573020, 10633020, 10673012, and 10603006 and by National Basic Research Program of China (973 Program) No. 2007CB815403.

REFERENCES

Armandroff, T. E. 1989, AJ, 97, 375
Ashman, K. A., Bird, C. M., & Zepf, S. E. 1994, AJ, 108, 2348
Barmby, P., & Huchra, J. 2001, AJ, 122, 2458
Barmby, P., Huchra, J., Brodie, J., Forbes, D., Schroder, L., & Grillmair, C. 2000, AJ, 119, 727
Bekki, K., Yahagi, H., & Forbes, D. A. 2007, MNRAS, 377, 215
Brodie, J. P., & Huchra, J. P. 1991, ApJ, 379, 157
Brodie, J., & Strader, J. 2006, ARA&A, 44, 193
Chandar, R., Ford, H. C., & Tsvetanov, Z. 2001, AJ, 122, 1330
Chandar, R., Whitmore, B., & Lee, M. G. 2004, ApJ, 611, 220
Côté, P. 1999, AJ, 118, 406
Eggen, O. J., Lynden-Bell, D., & Sandage, A. R. 1962, ApJ, 136, 748
Elson, R. A., & Walterbos, R. A. M. 1988, ApJ, 333, 594
Forbes, D. A., Brodie, J. P., & Larsen, S. S. 2001, ApJ, 556, L83
Freedman, W. L., Wilson, C. D., & Madore, B. F. 1994, ApJ, 427, 628
Frenk, C. S., & White, S. D. M. 1982, MNRAS, 198, 173
Gebhardt, K., & Kissler-Patig, M. 1999, AJ, 118, 1526
Harris, W. E., Whitmore, B. C., Karakla, D., Okoń, W., Baum, W. A., Hanes, D. A., & Kavelaars, J. J. 2006, ApJ, 636, 90

Huchra, J., Stauffer, J., & van Speybroeck, L. 1982, ApJ, 259, L57
Huchra, J. P., Brodie, J. P., & Kent, S. M. 1991, ApJ, 370, 495
Kong, X., et al. 2000, AJ, 119, 2745
Kundu, A., & Whitmore, B. C. 2001, AJ, 121, 2950
Larsen, S. S., Brodie, J. P., Huchra, J. P., Forbes, D. A., & Grillmair, C. J. 2001, AJ, 121, 2974
Ma, J., Zhou, X., Burstein, D., Chen, J., Jiang, Z., Wu, Z., & Wu, J. 2006, PASP, 118, 98
Ma, J., Zhou, X., Chen, J., Wu, Z., Yang, Y., Jiang, Z., & Wu, J. 2005, PASP, 117, 256
Mieske, S., et al. 2006, ApJ, 653, 193
Minniti, D. 1995, AJ, 109, 1663
Parmentier, G., & Gilmore, G. 2001, A&A, 378, 97
Parmentier, G., Jehin, E., Magain, P., Neuforge, C., Noels, A., & Thoul, A. A. 1999, A&A, 352, 138
Peng, E. W., et al. 2006, ApJ, 639, 95
Perelmuter, J. M., Brodie, J. P., & Huchra, J. 1995, AJ, 110, 620
Perrett, K. M., et al. 2002, AJ, 123, 2490
Perelmuter, J. M., & Racine, R. 1995, AJ, 109, 1055
Schroder, L. L., Brodie, J. P., Kissler-Patig, M., Huchra, J. P., & Phillips, A. C. 2002, AJ, 123, 2473
Searle, L., & Zinn, R. 1978, ApJ, 225, 357
Sharov, A. S. 1988, Soviet Astron. Lett., 14, 339
Spitler, L. R., Larsen, S. S., Strader, J., Brodie, J. P., Forbes, D. A., & Beasley, M. A. 2006, AJ, 132, 1593
Strader, J., Brodie, J. P., Spitler, L., & Beasley, M. A. 2006, AJ, 132, 2333
van den Bergh, S. 1969, ApJS, 19, 145
West, M. J., Côté, P., Marzke, R. O., & Jordan, A. 2004, Nature, 427, 31
Zepf, S. E., & Ashman, K. A. 1993, MNRAS, 264, 611
Zinn, R. 1985, ApJ, 293, 424